Polynomial-Method-based SIMO Controller Design for A Double Inverted Pendulum

Yue Qiao
Univ. of Michigan-Shanghai Jiao Tong Univ. Joint Institute,
Shanghai Jiao Tong University,
Shanghai, P. R. China
Email: chimmy@sjtu.edu.cn

Lin Zhou
Univ. of Michigan-Shanghai Jiao Tong Univ. Joint Institute,
Shanghai Jiao Tong University,
Shanghai, P. R. China
Email: automanzl@gmail.com

Chengbin Ma*
Univ. of Michigan-Shanghai Jiao Tong Univ. Joint Institute,
Shanghai Jiao Tong University,
Shanghai, P. R. China
Email: chbma@sjtu.edu.cn

***Abstract*—In this paper, a state feedback controller is designed via polynomial method for a double inverted pendulum. The polynomial method is first extended into state space. Then based on the equations of motion, the linearized state space model of double inverted pendulum is derived near the upright balance position. The state feedback controller is designed via polynomial method where Ackermann's formula is used to determined the gain matrix. The polynomial-method-based controller design is validated through real experiments. It is shown that the existence of closed-loop zeros in the overall control system imposes limit on the selection of the time constant in polynomial method. In the end, the performance of the controller design is compared with the well-known linear quadratic regulator control. The two controllers share an identical state feedback control configuration, but their design procedures are different. It is found that the two different control methods have a similar performance. However compared with the trial-and-error-based linear quadratic regulator optimal control, polynomial method is much more straightforward in terms of its design procedure due to clear physical meanings of its control parameters.**

I. Introduction

An inverted pendulum is a typical open-loop unstable system. The control of the inverted pendulum is a practical benchmark problem. Its application can be found in many real systems such as guidance systems on rockets and walking robots. Usually a double inverted pendulum (DIP) is a starting point for discussing the control of more complicated multi-link inverted pendulums. In DIP, there are two linked pendulums on a cart. Compared to the simplest single inverted pendulum (SIP), DIP is a higher-order single-input-multi-output (SIMO) system. Both of its two pendulums should be brought from the unstable position to the upright position only by the horizontal motion of the cart. DIP system is difficult to stabilize, and its controller design provides convincing evidence of the effectiveness of a design approach.

Many control methods both in the classical and modern control have been applied to the control of SIP and DIP. In 1970s, Bryson and Luenberger discussed the linear feedback and observer design of SIP via pole placement [1]. The classical control of SIP and DIP includes Lundherg and Roberge's research on stabilizing compensator using the root locus and Nyquist plot of the system [2]. Optimal control algorithms such as the well-known linear quadratic regulator (LQR) are widely used for linear DIP controller design [3]-[5]. High-order controllers in modern control were also proposed using H_∞ and μ-synthesis theories [6][7]. Adaptive sliding-mode control can also be applied for the stabilizing and tracking of a dual-axis inverted pendulum [14]. Recently the intelligent control including neural-network and fuzzy control becomes popular for the control of inverted pendulums [8]-[13] because the control is less dependent on accurate physical models. At the same time, in real applications, there are many limitations such as in the cost and performance of hardware, unavoidable on-site tuning, debugging effort and time. Therefore the low-order linear controllers are still dominant in industrial applications. Further improvement on the low-order controller design is both theoretically and practically important.

Besides the well-known classical and modern control, there is an alternative approach called polynomial method. In this method, the control configuration is predefined and thus the corresponding closed-loop characteristic polynomial can be derived at the beginning. Then the control parameters are determined via proper assignments of so-called characteristic ratios and time constant [15]. Naslin empirically observed the relationship between characteristic ratios and transient response in 1960s [16]. An important contribution is attributed to Manabe, who proposed the Coefficient Diagram Method (CDM) based on Naslin's findings and the Lipatov-Sokolov stability criterion [17]. By using CDM, he successfully designed controllers for many industrial applications [18]. Recently the polynomial method has been extended to new applications such as the force control of a flexible robot system [19].

In polynomial method, the design parameters have clear and different physical meanings. This advantage enables a straightforward design procedure. Furthermore, polynomial method uses closed-loop characteristic polynomial. In terms of closed-loop response, different low-order controllers may be actually equivalent with some basic control configurations such as the PID and state feedback configurations. Therefore the controller design and analysis using the polynomial method could become a general approach that does not depend on a specific control configuration. Based on the above basic consideration, this paper explores the possibility of the DIP single-input-multi-output (SIMO) controller design via polynomial method, while most existing research on polynomial method is based on the single-input-single-output (SISO) transfer functions. In the paper, the state space model of a DIP is firstly derived, and the corresponding state feedback controller is designed via polynomial method. The controller design

is then validated by real experiments. Thanks to the clear physical meanings of the control parameters in polynomial method, the classical tradeoff between speed of response and damping is explicitly represented. Finally the performance of polynomial-method-based controller design is compared with that of the well-known LQR optimal control. It is found that the two methods share a similar control performance, but the polynomial method is superior in terms of its straightforward design procedure.

II. Preliminary Discussion

For an initial discussion, an ideal all-pole closed-loop system is first analyzed,

$$G(s) = \frac{a_0}{a_n s^n + a_{n-1}s^{n-1} + ... + a_1 s + a_0}, \quad (1)$$

where a_i $(i = 0, 1, ..., n)$ are the coefficients of characteristic polynomial $P(s)$,

$$P(s) = a_n s^n + a_{n-1}s^{n-1} + ... + a_1 s + a_0. \quad (2)$$

In polynomial method, characteristic ratios γ_i $(i = 1, ..., n-1)$ and time constant τ are defined as follows:

$$\gamma_1 = \frac{a_1^2}{a_0 a_2},\ \gamma_2 = \frac{a_2^2}{a_1 a_3}, \ldots, \gamma_{n-1} = \frac{a_{n-1}^2}{a_{n-2} a_n}, \quad (3)$$

$$\tau = \frac{a_1}{a_0}. \quad (4)$$

Then characteristic polynomial $P(s)$ can be rewritten as

$$\frac{1}{\gamma_{n-1}\gamma_{n-2}^2 \cdots \gamma_1^{n-1}}(\tau s)^n + ... + \frac{1}{\gamma_1}(\tau s)^2 + (\tau s) + 1, \quad (5)$$

Based on the above equation, it is straightforward from Laplace transform that the time response is scaled by the factor τ, while the shape of the response (i.e. the stability and damping of the system) is determined only by the characteristic ratios.

Nonovershooting step response is of interest to determine a nominal assignment of γ_i's. It has been proved that an all-pole system has monotonous decreasing frequency response under the condition that all the characteristic ratios are larger than two [15]. Besides, a characteristic ratio with lower-index has a stronger influence [20]. Therefore overshoot can be adjusted by only changing γ_1. The minimum values of γ_1, γ_1^*'s, that enable nonovershootting response are listed in Table. I, which are determined numerically due to the difficulty in finding exact analytical solutions for high-order systems. The corresponding step responses are shown in Fig. 1.

It is interesting to notice that for systems with different orders, γ_1^*'s are all close to 2.5. This result well matches the standard form in CDM method which is based on intensive experimental studies [15][17]. Therefore a nominal assignment of characteristic ratios can be approximately determined as

$$\gamma_1 = 2.5 \text{ and } \gamma_i = 2 \text{ for } i = 2, ..., n-1. \quad (6)$$

With a fixed characteristic ratio assignment, the time response of an all-pole system, i.e. the speed of response, is scaled by the time constant τ, as shown in Fig. 1(b). In polynomial method, the clear physical meanings of the parameters, γ_i's and τ, enable a straightforward design procedure, as discussed in the following sections.

TABLE I. γ_1^*'s for nonovershooting step responses

Order of System	γ_1^*
3	2.61
4	2.53
5	2.48
6	2.48
7	2.48
8	2.48

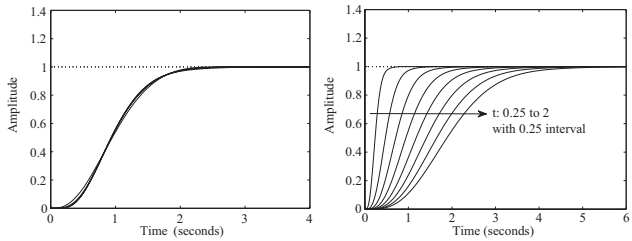

(a) (b)

Fig. 1. Step responses of the general all-pole closed-loop systems under the nominal characteristic ratio assignment. (a) Systems with the third to eighth orders and an identical τ(=1). (b) An example: the fifth-order system with various τ.

III. Extension to State Space

Besides using transfer functions such as (1), polynomial method can also be extend to design multi-input-multi-output (MIMO) controllers. The standard state space equations are represented as

$$\dot{\mathbf{X}} = \mathbf{AX} + \mathbf{BU},$$
$$\mathbf{Y} = \mathbf{CX} + \mathbf{DU}, \quad (7)$$

where $\mathbf{X} \in \mathbb{R}^n$, $\mathbf{Y} \in \mathbb{R}^q$, $\mathbf{U} \in \mathbb{R}^p$ and $\mathbf{A},\ \mathbf{B},\ \mathbf{C},\ \mathbf{D}$ are constant matrices with appropriate dimensions.

The state feedback control configuration shown in Fig. 2 is widely used in state-space-based controller design,

$$\mathbf{U} = \mathbf{R} - \mathbf{KX}, \quad \mathbf{K} \in \mathbb{R}^{p \times n} \quad (8)$$

where $\mathbf{K}$ is the gain matrix of the controller and $\mathbf{R}$ is the reference input. Combining (7) and (8), the overall transfer

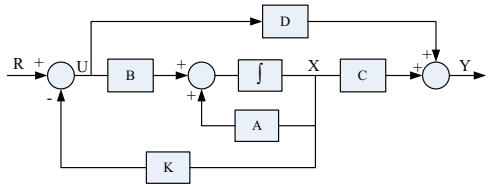

Fig. 2. Block diagram of a state feedback controller

matrix between the reference command and the output can be derived as

$$\mathbf{Y} = (\mathbf{C} - \mathbf{DK})(s\mathbf{I} - \mathbf{A} + \mathbf{BK})^{-1}\mathbf{BR} + \mathbf{DR}. \quad (9)$$

A matrix $\mathbf{M} \in \mathbb{R}^{n \times n}$ is defined as

$$\mathbf{M} = s\mathbf{I} - \mathbf{A} + \mathbf{BK}. \quad (10)$$

Then the transfer matrix can be simplified as

$$\mathbf{Y} = \frac{adj(\mathbf{M})(\mathbf{C} - \mathbf{DK})\mathbf{B} + det(\mathbf{M})\mathbf{D}}{det(\mathbf{M})}\mathbf{R}, \quad (11)$$

where $adj(\mathbf{M})$ is the adjoint matrix of $\mathbf{M}$ and $det(\mathbf{M})$ is the determinant of $\mathbf{M}$.

In (11), $\mathbf{A}$, $\mathbf{B}$, $\mathbf{C}$, $\mathbf{D}$ are constant matrices, and only matrix $\mathbf{M}$ contains the Laplace operator s. The determinant of $\mathbf{M}$ and the elements in the adjoint matrix of $\mathbf{M}$ are all polynomials of s. The determinant of $\mathbf{M}$ is actually the characteristic polynomial of the closed-loop system,

$$det(\mathbf{M}) = s^n + a_{n-1}(\mathbf{K})s^{n-1} + ... + a_1(\mathbf{K})s + a_0(\mathbf{K}). \quad (12)$$

The feedback gain matrix $\mathbf{K}$ can be designed via polynomial method to satisfy the characteristic ratio and time constant assignments,

$$\gamma_i = \frac{a_i^2(\mathbf{K})}{a_{i-1}(\mathbf{K})a_{i+1}(\mathbf{K})}, \quad \tau = \frac{a_1(\mathbf{K})}{a_0(\mathbf{K})}. \quad (13)$$

Under specific assignments of the characteristic ratios γ_i's and the time constant τ, the feedback gain matrix $\mathbf{K}$ can be determined by solving (13).

For a SIMO system, i.e. a special MIMO systems, the gain matrix $\mathbf{K}$ in the state feedback control can be uniquely determined by Ackermann's Formula with specific assignments of characteristic ratios and time constant.

$$\mathbf{K} = \mathbf{e}_n\mathbf{S}^{-1}\mathbf{P}(\mathbf{A}), \quad (14)$$

where $\mathbf{e}_n$ is the unit vector of dimension n and $\mathbf{S}$ is the controllability matrix,

$$\mathbf{e}_n = (0\ 0\ ...\ 0\ 1), \quad (15)$$

$$\mathbf{S} = [\mathbf{B}\ \mathbf{AB}\ \mathbf{A}^2\mathbf{B}\ ...\ \mathbf{A}^{n-1}\mathbf{B}]. \quad (16)$$

$\mathbf{P}(\mathbf{A})$ in (14) is a polynomial of matrix $\mathbf{A}$,

$$\mathbf{P(A)} = \mathbf{A}^n + a_{n-1}\mathbf{A}^{n-1} + a_{n-2}\mathbf{A}^{n-2} + ... + a_1\mathbf{A} + a_0\mathbf{I}, \quad (17)$$

where a_i is the the coefficients of a target characteristic polynomial designed under the assignment of the characteristic ratios γ_i's and a specific time constant τ. Based on (3)(4), the coefficient a_i in (17) can be solved as

$$\begin{cases} a_0 = \frac{\gamma_{n-1}\gamma_{n-2}^2\cdots\gamma_2^{n-2}\gamma_1^{n-1}}{\tau^n}, \\ a_1 = \frac{\gamma_{n-1}\gamma_{n-2}^2\cdots\gamma_2^{n-2}\gamma_1^{n-1}}{\tau^{n-1}}, \\ ... \\ a_i = \gamma_{n-1}\gamma_{n-2}^2\cdots\gamma_{i+1}^{n-i-1}(\frac{\gamma_i\cdots\gamma_2\gamma_1}{\tau})^{n-i} \quad i = 2, 3, ..., n-1. \end{cases} \quad (18)$$

IV. Control of Double Inverted Pendulum

Double inverted pendulum (DIP) is a typical benchmark SIMO system. Here the state feedback controller for a DIP in Fig. 2 is designed via polynomial method.

A. System modeling

As shown in Fig. 3, the DIP model consists of a cart, two pendulums and a free joint block. The notation and the parameter values are shown in Table. II. For the sake of simplicity, the pendulums are assumed to be uniform, and the free joint block is assumed to be dimensionless with mass m_3.

The equations of motion for the DIP system can be obtained using the Largrange equations with the generalized coordinates $\mathbf{q} = (\theta_1, \theta_2)$. The total kinetic energy K of the system relates to the motion of the cart, two pendulums and the joint block,

$$\begin{aligned} K = &\frac{1}{2}M\dot{x}^2 + \frac{1}{2}m_1\dot{x}^2 - m_1l_1\dot{x}\dot{\theta}_1cos\theta_1 + \frac{2}{3}m_1l_1^2{\dot{\theta}_1}^2 \\ &+ \frac{1}{2}m_2[\dot{x}^2 - 2\dot{x}(2l_1\dot{\theta}_1cos\theta_1 + l_2\dot{\theta}_2cos\theta_2)] \\ &+ \frac{1}{2}m_2[4l_1^2{\dot{\theta}_1}^2 + \frac{4}{3}l_2^2{\dot{\theta}_2}^2 + 4l_1l_2\theta_1\theta_2cos(\theta_1 - \theta_2)] \\ &+ \frac{1}{2}m_3\dot{x}^2 - 2m_3l_1\dot{x}\dot{\theta}_1cos\theta_1 + 2m_3l_1^2{\dot{\theta}_1}^2 \end{aligned} \quad (19)$$

The total potential energy V of the system can also be calculated as follows,

$$V = m_1l_1cos\theta_1 + m_2(2l_1cos\theta_1 + l_2cos\theta_2) + 2m_3l_1cos\theta_1. \quad (20)$$

Then combining (19) and (20), the Lagrangian L of the system can be represented as

$$L = K - V. \quad (21)$$

Since no external force is acted on the generalized coordinates θ_1 and θ_2, the equations of motion can be obtained by solving the Euler-Lagrange equation,

$$\frac{d}{dt}\frac{\partial L}{\partial\dot{\theta}_1} - \frac{\partial L}{\partial\theta_1} = 0, \quad (22)$$

$$\frac{d}{dt}\frac{\partial L}{\partial\dot{\theta}_2} - \frac{\partial L}{\partial\theta_2} = 0. \quad (23)$$

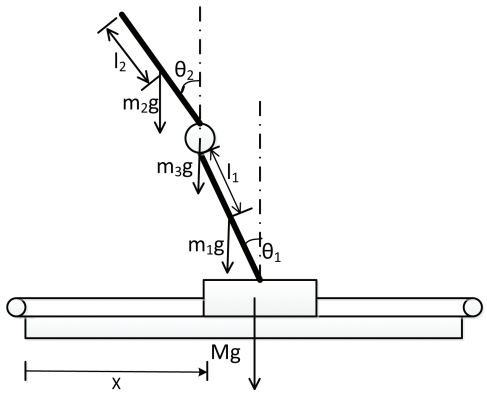

Fig. 3. Model of double inverted pendulum

TABLE II. Notations and parameter values for the DIP model

Notation	Description	Parameter value
M	mass of cart	1.1 kg
m_1	mass of lower pendulum	0.05 kg
m_2	mass of upper pendulum	0.132 kg
m_3	mass of free joint block	0.236 kg
l_1	distance form pin of cart to centre of gravity of lower pendulum l	0.0775 m
l_2	distance form pin of upper pendulum to centre of gravity of upper pendulum l	0.251 m
g	acceleration of gravity	9.8 m/s^2
x	linear displacement of the cart	
θ_1	angular displacement of the lower pendulum	
θ_2	angular displacement of the upper pendulum	

Applying (19)-(21) to (22) and (23), the equations of motion for the DIP are calculated as

$$6m_2l_2\theta_2l_2\dot{\theta_2}^2sin(\theta_2-\theta_1)+4(m_1+3m_2+3m_3)l_1\ddot{\theta_1} + 6m_2l_2\ddot{\theta_2}cos(\theta_2-\theta_1) + (m_1+2m_2+2m_3)(gsin\theta_1+\ddot{x}cos\theta_1)=0, \tag{24}$$

$$-3gsin\theta_2-6l_1\dot{\theta_1}^2sin(\theta_2-\theta_1)+4l_2\ddot{\theta_2}+3\ddot{x}[2l_1cos(\theta_2-\theta_1) - cos\theta_2]=0. \tag{25}$$

Equation (22) and (23) can be further linearized around the upright balance point, i.e., $(\theta_1,\ \theta_2)=(0,\ 0)$,

$$\ddot{\theta_1}=K_{11}\theta_1+K_{12}\theta_2+K_{13}\ddot{x}, \tag{26}$$

$$\ddot{\theta_2}=K_{21}\theta_1+K_{22}\theta_2+K_{23}\ddot{x}, \tag{27}$$

where

$$\begin{aligned} K_{11}&=\frac{3(m_1+2m_2+2m_3))g}{l_1(4m_1+3m_2+12m_3)},\\ K_{21}&=\frac{-9(m_1+2(m_2+m_3))g)}{2l_2(4m_1+3m_2+12m_3)},\\ K_{12}&=\frac{-9m_2g}{2l_1(4m_1+3m_2+12m_3)},\\ K_{22}&=\frac{3(m_1+3(m_2+m_3))g)}{l_2(4m_1+3m_2+12m_3)},\\ K_{13}&=\frac{3(2m_1+m_2-4m_3)}{2l_1(4m_1+3m_2+12m_3)},\\ K_{23}&=\frac{-3m_1}{2l_2(4m_1+3m_2+12m_3)}. \end{aligned} \tag{28}$$

The state space model for the DIP system is represented as

$$\begin{aligned} \dot{\mathbf{X}} &= \mathbf{AX}+\mathbf{B}U,\\ \mathbf{Y} &= \mathbf{CX}, \end{aligned} \tag{29}$$

where the input U, state vector $\mathbf{X}$ and output $\mathbf{Y}$ are defined as

$$U=\ddot{x}=a\cdots\cdots\cdots\text{acceleration of cart}, \tag{30}$$

$$\mathbf{X}=(x,\theta_1,\theta_2,\dot{x},\dot{\theta_1},\dot{\theta_2})^T,\quad \mathbf{Y}=(x,\theta_1,\theta_2)^T. \tag{31}$$

Then from (26) and (27), the coefficient matrices in (29) can be derived as

$$\mathbf{A}=\begin{pmatrix} 0&0&0&1&0&0\\ 0&0&0&0&1&0\\ 0&0&0&0&0&1\\ 0&0&0&0&0&0\\ 0&K_{11}&K_{12}&0&0&0\\ 0&K_{21}&K_{22}&0&0&0 \end{pmatrix},\quad \mathbf{B}=\begin{pmatrix} 0\\0\\0\\1\\K_{13}\\K_{23} \end{pmatrix},$$

$$\mathbf{C}=\begin{pmatrix} 1&0&0&0&0&0\\ 0&1&0&0&0&0\\ 0&0&1&0&0&0 \end{pmatrix}. \tag{32}$$

Substitution with the parameter values in Tab II yields

$$\mathbf{A}=\begin{pmatrix} 0&0&0&1&0&0\\ 0&0&0&0&1&0\\ 0&0&0&0&0&1\\ 0&0&0&0&0&0\\ 0&86.69&-21.62&0&0&0\\ 0&-40.31&39.45&0&0&0 \end{pmatrix},\ \mathbf{B}=\begin{pmatrix} 0\\0\\0\\1\\6.64\\-0.088 \end{pmatrix}. \tag{33}$$

$$\mathbf{Y}=\mathbf{C}(s\mathbf{I}-\mathbf{A})^{-1}\mathbf{B}U. \tag{34}$$

The characteristic equation can be derived as

$$det(s\mathbf{I}-\mathbf{A})=s^6-126.14s^4+2548.4s^2 \tag{35}$$

So the DIP is a typical unstable system with roots

$$r=(0,0,-5.03,5.03,-10.04,10.04) \tag{36}$$

On the other hand, the controllability matrix $\mathbf{S}$ of the system can be calculated as

$$\mathbf{S}=\begin{pmatrix} 0&1&0&0&0&0\\ 0&6.64&0&557.5&0&55927\\ 0&-0.088&0&-271.1&0&-33976\\ 1&0&0&0&0&0\\ 6.64&0&577.5&0&55927&0\\ -0.09&0&-271.1&0&-33976&0 \end{pmatrix}. \tag{37}$$

The DIP system is controllable because $\mathbf{S}$ is nonsingular.

B. Controller design

With the previously derived DIP model, the state feedback controller in Fig. 2 can be designed using polynomial method.

$$U=R-\mathbf{KX}. \tag{38}$$

Since DIP is a controllable SIMO system, U and R are both one dimension variables. Ackermann's formula can be applied to determine the gain vector $\mathbf{K}$. From the derived state space model of the DIP system, the matrix polynomial **P(A)** in Ackermann's formula has the order of six. As discussed above, the nominal characteristic ratio assignment in the DIP control is selected as $\gamma_i=[2.5,\ 2,\ 2,\ 2,\ 2]$. Based on (18), **P(A)** is solved as

$$\begin{aligned} \mathbf{P(A)} &= \mathbf{A}^6+\frac{40}{\tau}\mathbf{A}^5+\frac{800}{\tau^2}\mathbf{A}^4+\frac{8000}{\tau^3}\mathbf{A}^3+\frac{4\times10^4}{\tau^4}\mathbf{A}^2\\ &\quad+\frac{1\times10^5}{\tau^5}\mathbf{A}+\frac{1\times10^5}{\tau^6}\mathbf{I}. \end{aligned} \tag{39}$$

Finally combining (15), (37) and (39), the gain vector $\mathbf{K}$ can be solved as equations of the time constant τ.

$$\mathbf{K}=\mathbf{e}_n\mathbf{S}^{-1}\mathbf{P}(\mathbf{A})=[k_1\ k_2\ k_3\ k_4\ k_5\ k_6], \tag{40}$$

where

$$\begin{aligned} k_1&=\frac{3.92\times10^1}{\tau^6},\\ k_2&=\frac{1.18\times10^2}{\tau^2}-\frac{2.01}{\tau^4}-\frac{6.08}{\tau^6}+1.89\times10^1,\\ k_3&=\frac{-1.19\times10^2}{\tau^2}-\frac{1.52\times10^2}{\tau^4}-\frac{1.30\times10^1}{\tau^6}-9.08,\\ k_4&=\frac{3.92\times10^1}{\tau^5},\\ k_5&=\frac{5.91}{\tau}-\frac{4.20\times10^{-1}}{\tau^3}-\frac{6.08}{\tau^5},\\ k_6&=-\frac{5.95}{\tau}-\frac{3.04\times10^1}{\tau^3}-\frac{1.30\times10^1}{\tau^5}. \end{aligned} \tag{41}$$

The designed gain vectors $\mathbf{K}$ under different assignments of τ are shown in Table. III.

TABLE III. GAIN VECTOR OF DIP CONTROL VIA POLYNOMIAL METHOD

τ	K
0.9	[73.84, 151.16, -411.65, 66.45, -4.24, -70.19]
1.0	[39.24, 129.69, -292.76, 39.24, -0.54, -49.26]
1.2	[13.14, 98.44, -169.21, 15.77, 2.28, -27.73]
1.4	[5.21, 78.21, -110.99, 7.30, 2.97, -17.72]
1.6	[2.34, 64.65, -79.47, 3.74, 3.04, -12.36]
1.8	[1.15, 55.21, -60.62, 2.08, 2.91, -9.20]

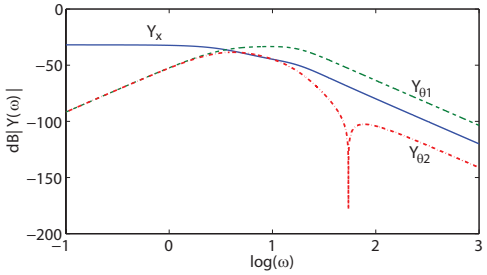

Fig. 4. Frequency responses of the closed-loop transfer matrix

C. Closed-loop frequency response

For the SIMO control of DIP system, the closed-loop transfer matrix between the reference input R and the output vector $\mathbf{Y}$ can be represented as

$$\mathbf{T} = \frac{\mathbf{Y}}{R} = \mathbf{C}(s\mathbf{I} - \mathbf{A} + \mathbf{BK})^{-1}\mathbf{B} \tag{42}$$

where

$$\mathbf{T} = [T_x,\ T_{\theta 1},\ T_{\theta 2}]. \tag{43}$$

$$T_x = \frac{x}{R},\quad T_{\theta 1} = \frac{\theta_1}{R},\quad T_{\theta 2} = \frac{\theta_2}{R} \tag{44}$$

With the derived gain vector $\mathbf{K}$ in (40)(41), the frequency responses of T_x, $T_{\theta 1}$ and $T_{\theta 2}$ can be calculated as shown in Fig. 4, where the τ is selected to be 1. According to the frequency response of T_x, the reference input R would leads to the nonzero steady state for x. While the steady states for θ_1 and θ_2 are always zeros for the reason that $\theta_1 = \theta_2 = 0$ is the only balance condition for DIP system. Considering that in steady-state, the input U in (38) should be zero, the steady state of x can be easily determined as

$$x_{ss} = \frac{1}{k_1} \cdot R, \tag{45}$$

.

It has already been shown that the gain vector $\mathbf{K}$ changes with different assignment of time constant τ (see (41)). Even though the nominal assignments of characteristic ratios are always available by proper design of $\mathbf{K}$ in (42), due to the existence of system zeros, the damping of closed-loop system is also influenced by the assignment of time constant. Since the output x has nonzero steady state in (45), frequency responses of T_x with different time constant assignment is analyzed. Normalization can be held by letting

$$T_x^* = k_1 T_x, \tag{46}$$

so that the transfer function T_x^* has unitary steady-state gain. Due to the complexity of high-order system zeros in (42), numerical simulations are demonstrated in Fig. 5. A clear

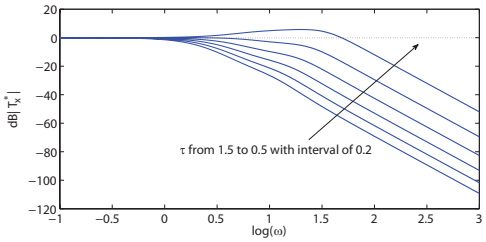

Fig. 5. Frequency response of T_x^* with the change of time constant

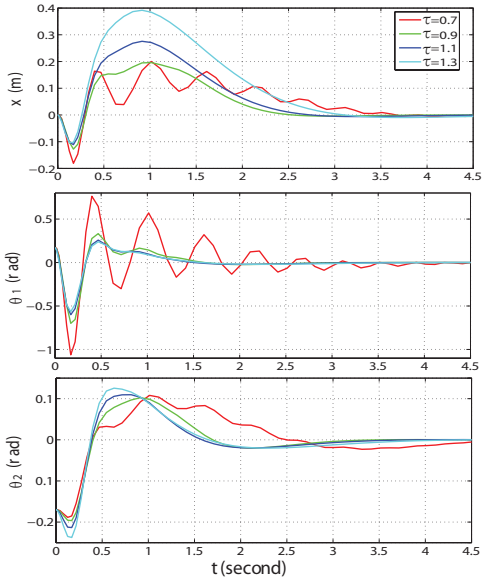

Fig. 6. Simulation results of disturbance response with different time constants

trade-off between response speed and damping can be observed. With the increasing of response speed, i.e, decreasing of time constant τ, the damping of system drops gradually. And the further decreasing of τ finally leads to the appearance of resonant peak in frequency response.

D. Simulation of disturbance response

Considering that DIP is only balanced at the upright position, disturbance response is analyzed for system with angle bias. The following simulations look into the case that both pendulums have an angle bias of 0.17 rad(10 degree) in opposite directions.

As shown in Fig 6, we can see that the angle disturbance can be well suppressed to move the system output to steady state. Meanwhile, the response speed of the system slows down as τ increases. It can be observed that the fast response with small value of τ has poor system damping due to the existence of system zeros as mentioned. Therefore, the response speed has certain limitations considering the disturbance response.

V. EXPERIMENTAL RESULTS

The designed controllers are implemented using a Googol GLIP2002 DIP test bench, shown in Figs. 7 and 8. The DIP test bench in Fig. 8 consists of a base, a chart, two pendulum

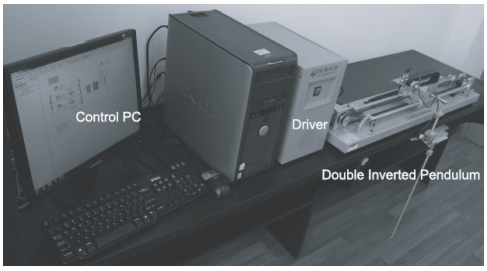

Fig. 7. Experimental setup

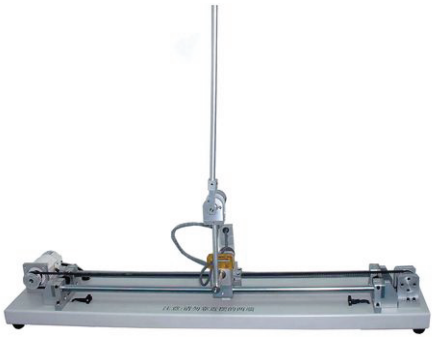

Fig. 8. The double inverted pendulum

rods and a servomotor. The cart is driven by the servomotor through the timing belt to move back and forth on the sliding shaft. Three optical encoders send feedback signals including the cart displacement and the angular displacements of the two pendulums.

The inverted pendulum system is controlled by a PC equipped with a DSP-based motion control card (GT-400-SV-PCI) with advanced data I/O and storage capability. The controller is executed in MATLAB Simulik by using the Real-Time Workshop (RTW) Toolbox. During the experiment, if any one of pendulum angles is exceed 35 degree, the system will automatically stop for safety.

A. Polynomial-based design

The experimental results using the designed controllers in Table. III are shown in Fig. 9. For a fast response with $\tau = 0.9$, the control system becomes unstable due to the lack of damping. The existence of closed-loop zeros in state feedback control, i.e. in (11), impose limits on the selection of a desired response speed, i.e. the time constant τ. The experimental results well reflect the classical tradeoff between damping and response speed in controller design.

B. Comparison with linear quadratic regulator

Linear quadratic regulator (LQR) is a common optimal control in state space. Various LQR-based controllers have already proposed for single inverted pendulum (SIP) control [21][22]. In this paper, for a purpose of comparison, the state feedback controller for the DIP is also designed using LQR optimal control. After a considerable amount of trial-and-error in simulation, a satisfactory LQR weighting matrix is

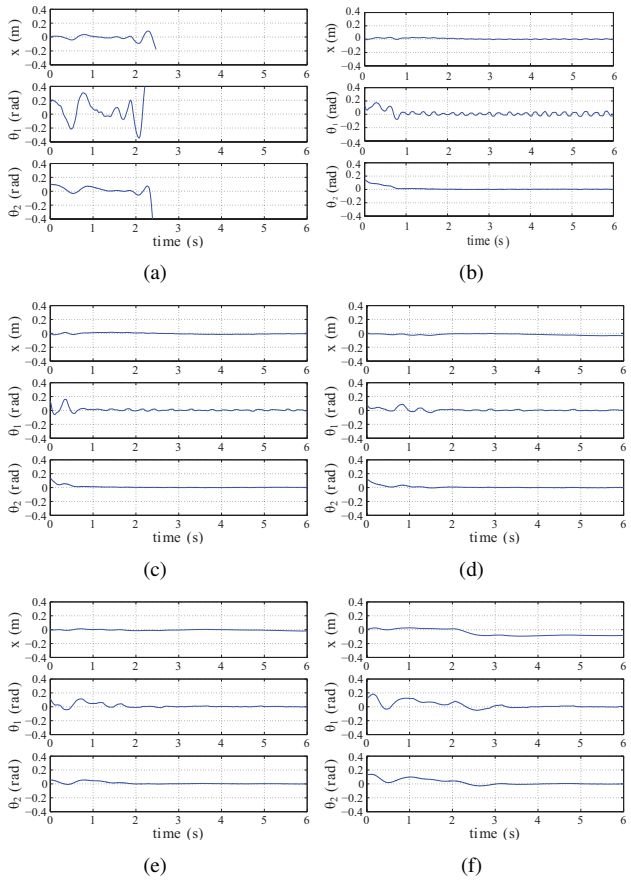

Fig. 9. Experimental results using different time constants. (a)$\tau = 0.9$. (b)$\tau = 1.0$. (c)$\tau = 1.2$. (d)$\tau = 1.4$. (e)$\tau = 1.6$. (f)$\tau = 1.8$.

determined, as shown in Table IV. Then the feedback gain vector $\mathbf{K}$ can be determined accordingly,

$$\mathbf{K} = [17.32,\ 110.87,\ -197.57,\ 18.47,\ 2.71,\ -32.14]. \quad (47)$$

The corresponding characteristic ratios and time constant can be calculated as

$$\begin{aligned} \gamma_i &= [2.1908, 2.0938, 1.9191, 1.9883, 2.3913], \\ \tau &= 1.063. \end{aligned} \quad (48)$$

TABLE IV. WEIGHTING MATRIX OF LQR OPTIMAL CONTROL

Weighting matrix	Value
Q	[300, 500, 500, 0, 0, 0]
R	1

Since the time constant in LQR is 1.063, for a comparison purpose, the time constant in (41) is also set to be 1.063. The experimental results of LQR and polynomial-method-based controllers are demonstrated in Fig. 10. The control performances of the two controllers are similar. It is well known that LQR controller design is a mathematical approach which is based on intensive trail-and-error to determine the weighting matrix. Compared with LQR control, polynomial method is an analytic procedure which is a more straightforward approach. The similar control performance indicates that polynomial method is an efficient analytical way to approach the optimum.

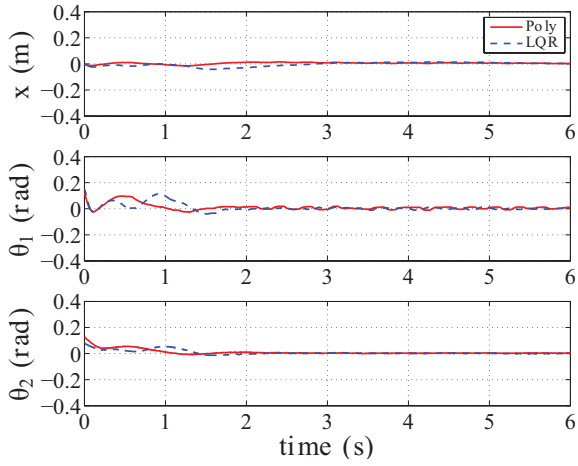

Fig. 10. Performance comparison between the polynomial-method-based controller and the LQR controller.

VI. Conclusion

In this paper, the state feedback control of a DIP system is designed via the polynomial method. The linearized state space model of the DIP is firstly derived from the equations of motion. The control parameters are then determined through nominal characteristic ratio assignment under different response speeds, i.e. assignment of τ. The designed controllers are validated using real experiments. It is found that the existence of the zeros imposes limit on the selection of response speed, i.e. τ. According to the experimental results, with an increasing response speed, once its corresponding time constant τ is smaller than 0.9, the damping of the system becomes insufficient.

The polynomial-method-based control is also compared with the well-known LQR optimal control. The two controllers share an identical control configuration, but different design approach. It is interesting to find that the optimization-based LQR control actually results characteristic ratios close to the nominal assignment in the polynomial method. The two design approaches have a similar performance in the experiments. However the polynomial-method-based controller design is a more straightforward analytical design, while the LQR control of the DIP heavily depends on intensive trial-and-error-based selection of the weighting matrix. Compared to the LQR control, polynomial method is a general and effective approach because its control parameters have clear physical meanings. This unique advantage would make it suitable for solving real control problems.

Acknowledgment

The authors would like to thank National Science Foundation of China, for supporting this work [grant number 50905113 (2010-2012)].

References

[1] A. E. Bryson and D. G. Luenberger, "The synthesis of regulator logic using variable control", *Proceeding of the IEEE*, vol. 58, no. 11, pp .1803-1811, 1970.

[2] K. H. Lundherg and J. K. Roberge, "Classical dual-inverted-pendulum control", *Proceedings of the 42nd IEEE Conference on Decision and Control*, pp. 4399-4404, NJ, USA, 2003.

[3] M. J. Anderson and W. J. Grantham, "Lyapunov optimal feedback control of a nonlinear inverted pendulum", *Trans ASME*, vol. 111, pp. 554-558, 1989.

[4] A. Bogdanov, "Optimal control of a double inverted pendulum on a cart", *Technical Report CSE-04-006, OGI School of Science and Engineering*, OHSU, 2004.

[5] X. Xiong and Z. Wan, "The simulation of double inverted pendulum control based on particle swarm optimization LQR algorithm", *IEEE International Conference on Software Engineering and Service Sciences*, pp. 253-256, Jul. 2010.

[6] G. van der Linden and P. Lambrechis, "H_∞ control of an experimental inverted pendulum with dry friction", *IEEE Contr. Syst. Mag.*, vol. 13, no. 4, pp. 44-50, 1993.

[7] H. Niemann and J. K. Poulsen, "Analysis and design of controllers for a double inverted pendulum", *Proceeding of American Control Conference*, pp. 2903-2908, Denver, CO, USA, 2003.

[8] C. W. Anderson, "Learning to control an inverted pendulum using neural networks", *IEEE Contr. Syst. Mag.*, vol. 9, pp. 31-37, Apr. 1989.

[9] V. William and L. Matsuoka, "Learning to balance the inverted pendulum using neural networks", *Proceeding of IEEE Int. Conf. Robotics and Automation*, vol. 3, pp. 2644-2649, 1991.

[10] S. Jung and S. S. Kim, "Control experiment of a wheel-driven mobile inverted pendulum using neural network", *IEEE Trans. Control Systems Technology*, vol. 16, no. 2, pp. 297-303, 2008.

[11] T. Yamakawa, "Stabilization of an inverted pendulum by a high-speed fuzzy logic controller hardware system", *Fuzzy Sets and Systems, Elsevier*, vol. 32, no. 2, pp. 161-180, Sep. 1989.

[12] S. Lei and R. Langari, "Hierarchical fuzzy logic control of a double inverted pendulum", *Proceeding of IEEE Int. Conf. on Fuzzy Syst.*, San Antonio, TX, pp. 1074-1077, 2000.

[13] L. Wang, S. Zheng, X. Wang, and L. Fan, "Fuzzy control of a double inverted pendulum based on information fusion", *Proceeding of International Conf. on Intelligent Control and Information Processing*, pp. 327-331, 2010.

[14] R. J. Wai and L. J. Chang, "Adaptive stabilizing and tracking control for a nonlinear inverted-pendulum system via sliding-mode technique", *IEEE Trans. Ind. Electron.*, vol. 53, no. 2, pp. 674-692, Apr. 2006.

[15] Y. C. Kim, L. H. Keel, and S. P. Bhattacharyya, "Transient response control via characteristic ratio assignment", *IEEE Trans. Automatic Control.*, vol. 48, no. 12, pp. 2238-2244, Dec. 2003.

[16] P. Naslin, "Essentials of optimal control", Cambridge, MA: Boston Technical Publishers, Inc., 1969.

[17] S. Manabe, "Importance of coefficient diagram in polynomial method", *Proceeding of the 42nd IEEE Conference on Decision and Control*, Maui, Hawaii USA, pp. 3489-3494, 2003.

[18] K. S. R. Hirokawa and S. Manabe, "Autopilot design for a missile with reaction-jet using coefficient diagram method", *Proceeding of AIAA Guidance, Navigation and Control Conference*, Montreal, Canada, pp. 1C8, 2001.

[19] C. Mitsantisuk, M. Nandayapa, K. Ohishi, and S. Katsura, "Resonance ratio control based on coefficient diagram method for force control of flexible robot system", *Proceeding of 12th IEEE International Workshop on Advanced Motion Control,*, pp. 1C6, 2012.

[20] Y. Kim, K. Kim, and S. Manabe, "Sensitivity of Time Response to Characteristic Ratios", *IEICE Trans. Fundamentals*, vol. E89-A, no. 2, Feb. 2006.

[21] A. N. K. Nasir, M. A. Ahmad and M. F. Rahmat, "Performance comparison between LQR and PID controller for an inverted pendulum system", *Proceeding of Int. Conf. on Power, Control and Optimization*, vol. 1052, pp. 124 - 128, Oct. 2008.

[22] X. Chen, H. Zhou, R. Ma, F. Zuo, G. Zhai, and M. Gong,, "Linear motor driven inverted pendulum and lqr controller design", *Proceeding of the IEEE International Conference on Automation and Logistics*, pp. 1750 - 1754, Jinan, China, Aug. 2007.